

Experimental and theoretical study of adiabatic, intermediate, and isothermal oscillations in air

J. Pierrus and O. L. de Lange

Department of Physics, University of Natal, Private Bag X01, Scottsville Pietermaritzburg 3209, South Africa

(Received 25 November 1996)

We have used an electronic technique in R uchardt's experiment to obtain accurate measurements of oscillations in air confined to a finite volume at room temperature and pressure. The dimensions of the container are small compared to the wavelength of sound for the frequencies used (0.5 to 8 Hz). The nature of the oscillations depends on both frequency and amplitude. Below about 2 Hz, the oscillations undergo several changes as their amplitude decreases due to damping: (i) an initial adiabatic oscillation is followed by (ii) a transition (lasting one or two cycles) to intermediate oscillations which persist for several cycles, until the amplitude has decreased to a few mm, when there is (iii) a second, larger transition, (lasting two or three cycles) to (iv) isothermal oscillations which persist until the motion ceases. Above 2 Hz we cannot distinguish the initial adiabatic oscillation, and the oscillations are all of the same intermediate type. A theoretical model is presented for the effects of heat conduction on the bulk modulus of the gas and the relaxation time of the initial intermediate oscillations, and these are compared with measured values. [S1063-651X(97)08009-4]

PACS number(s): 51.30.+i, 03.40.-t, 05.60.+w

I. INTRODUCTION

The work reported here is an experimental and theoretical study of various oscillations, and the associated heat flows, in a gas (air) which is confined in a finite volume. It has been known for almost two centuries that the physical phenomena associated with oscillations in a gas depend on the nature of the heat flows (even in an infinite medium). In fact, this feature was encountered earlier, at the dawn of Newtonian physics: in the second edition of the *Principia*, Newton compared his calculated value of the speed of sound in air with the measured value and found a discrepancy of almost 17% [1]. Subsequently it emerged from the work of Lagrange, Laplace, Poisson, and others, that Newton's value applies to isothermal vibrations where the temperature of the gas is maintained at a constant value by thermal conduction within the gas, whereas sound vibrations in air are adiabatic, with no internal heat transfer [2]. The relation between the velocities in these two limits was shown to be $c_a = \sqrt{\gamma} c_i$ where γ is the usual ratio of specific heats of the gas $\gamma = C_p/C_v$.

Attention soon turned to some general questions concerning this phenomenon, such as, under what conditions do the limiting adiabatic and isothermal oscillations obtain, and what are the properties of the oscillations between these extremes? For example, in 1851 Stokes published a study in which he supposed that the heat transfer is due to radiation rather than conduction. He concluded that sound waves of sufficiently low frequency in a gas would travel isothermally whereas waves of high frequency would propagate adiabatically [3]. It was later recognized that the heat flow is predominantly conductive, and it was shown that, at least for an unbounded medium, Stokes' conclusion is incorrect: sound waves of low frequency are adiabatic and become isothermal only at very high frequency [2]. This results from two competing influences: (i) the time available for heat flow between neighboring regions of compression and rarefaction in the wave increases as the frequency decreases. But, (ii) the scale for the distance that this heat has to be conducted is set by the wavelength, and this increases with decreasing fre-

quency. That is, a competition between the rate at which heat is transported by the wave and the rate of diffusion of heat by conduction. At low frequencies the former effect dominates and the vibrations are adiabatic; at sufficiently high frequencies the opposite is true and the vibrations are isothermal [2,4]. Here low and high frequency means small or large compared with a characteristic frequency

$$f_c = c_a^2 / 2\pi\kappa, \quad (1)$$

where

$$\kappa = \lambda / \rho C_p \quad (2)$$

is the thermal diffusivity [2]. (λ and ρ denote the thermal conductivity and the equilibrium density of the gas.) For gases under standard conditions the frequency (1) is high, for example, for air $f_c \sim 10^9$ Hz.

Stokes also considered the effect of heat transfer on the attenuation of sound waves, and found that adiabatic and isothermal waves would propagate with little attenuation, whereas waves between these extremes would be strongly damped [3]. These conclusions are essentially correct, at least if viscous contributions are negligible; the latter may contribute significantly at frequencies above f_c [2,5].

In the above, no account is taken of the influence of boundaries to the medium on the dynamics of the gas. Such effects can be of considerable importance in, for example, the flow of fluids in pipes, and the occurrence and properties of adiabatic, isentropic, and isothermal flows have been exhaustively studied [6], and will not be referred to again in this paper. For the oscillations of confined gases the effect of the walls has also been considered, for example, to determine the corrections that must be applied to measurements of the velocity of sound and the ratio of specific heats γ [7]. Larger effects are known for sound waves in porous materials where the oscillations can become isothermal if the pores are sufficiently small [8]. The essential physics of these effects is the following. Suppose that an oscillation in the volume of the gas is induced by an oscillation in (part of) the wall of the

container. (This is made more specific later in the paper.) Consider that the frequency of the oscillation, or the volume of the container, or both, are sufficiently low that the wavelength is much greater than the dimensions of the container. (For example, the wavelength of a 1 Hz vibration exceeds the dimensions of a typical container, $\sim 0.01\text{--}1$ m, by more than two orders of magnitude.) If the oscillation of the gas is purely adiabatic then the temperature of the gas will oscillate uniformly about its ambient value. But, due to the finite thermal conductivities of the gas and the walls, and because the length scale for thermal conduction is now set by the dimensions of the container, there will be superimposed on this adiabatic temperature oscillation a nonuniform, time-dependent contribution (see Sec. IV). For the initial departure from an adiabatic oscillation, the effect of heat conduction on certain physical properties, such as the bulk modulus and measurements of γ , is also small. In the extreme case where the adiabatic temperature variation is nullified by thermal conduction into and out of the walls, the oscillation is isothermal. We refer to oscillations which are not at the adiabatic or isothermal extremes, as intermediate.

There are a number of questions one may ask here, and these are the motivation for our work. (i) What is a suitable experimental procedure for detecting the expected transitions from adiabatic to intermediate to isothermal oscillations in a confined gas? (ii) Apart from obvious physical variables such as the frequency, volume and thermal conductivities, on what additional variables do the transitions depend? For example, how does the amplitude of the oscillation affect the transitions? (iii) What changes in dissipation occur during these transitions? (iv) Can one, with the aid of a theoretical model, identify the contributions of heat flow to the bulk modulus and the total dissipation?

In Sec. II we describe how modification of a well-known experiment provides a simple experimental procedure for answering these questions. The results of our experiments on air are presented and discussed in Sec. III. In Sec. IV a theoretical model is described for the effect of heat conduction on the bulk modulus of the gas and the relaxation time of the oscillations, and the results of the model are compared with measured values.

II. EXPERIMENTAL PROCEDURE

The experiment which suits our purposes is the well-known experiment Rüchardt [9] used in 1929 to measure the ratio of specific heats of gases and which has since become a standard teaching experiment. The apparatus consists of a glass aspirator with a stopper through which passes a precision-made glass tube. A closely fitting smooth steel ball is placed in the tube. If the ball is displaced from its equilibrium position and released, it performs a weakly damped, simple harmonic motion. By measuring the period of this motion a value of γ can be obtained [9].

It will be useful for what follows to briefly recall the theory of this experiment. Let m denote the mass of the ball, x the displacement of the ball from its equilibrium position, and ΔP_x the corresponding change in the pressure of the gas. The restoring force on the ball is

$$F_r = A \Delta P_x, \quad (3)$$

where A is the cross-sectional area of the tube. For small oscillations

$$\Delta P_x = -K \Delta V/V, \quad (4)$$

where K is the bulk modulus of the gas, V is its equilibrium volume, and $\Delta V = Ax$. It is assumed that the frictional force is proportional to the speed of the ball

$$F_d = -\beta \dot{x}, \quad (5)$$

where β is a constant. Then the equation of motion for small oscillations of the ball is

$$m\ddot{x} + \beta\dot{x} + (KA^2/V)x = 0. \quad (6)$$

Consequently

$$x(t) = X e^{-t/\tau} \cos 2\pi t/T, \quad (7)$$

where X is the initial displacement,

$$\tau = m/2\beta \quad (8)$$

is the relaxation time, and

$$T = \left(\frac{4\pi^2 mV}{KA^2} \right)^{1/2} \quad (9)$$

is the period of the oscillation. (In our work the damping is sufficiently weak that the difference in period between the damped and undamped oscillations is negligible, see below.) In the usual application of this experiment it is assumed that the gas is perfect and the oscillations are adiabatic. Then $K = \gamma P$, where P is the equilibrium pressure of the gas. The period T is measured as the average of a number of cycles, and Eq. (9) is used to obtain γ [9–11].

It is clear that Rüchardt's experiment provides a means for monitoring both the bulk modulus of the gas and the total relaxation time during the oscillations, from accurate measurements of $x(t)$. These two observations allow one to determine whether the nature of the oscillation is changing, and to detect any accompanying change in dissipation. For example, for isothermal oscillations of a perfect gas, $K = P$ and the period (9) is a factor $\sqrt{\gamma}$ greater than the adiabatic value; for air ($\gamma = 1.40$) this is about an 18% increase, and it should therefore be readily measurable by an electronic technique. The use of such a technique to measure $x(t)$ is our main modification of Rüchardt's experiment and we now proceed to describe it.

A block diagram of the apparatus is shown in Fig. 1(a). Here L1 and L2 represent coils (the excitation coils) which are wound in opposite senses, but are otherwise identical. They are mounted coaxially with the glass tube. A third coil, L3 (the pick-up coil), also mounted coaxially, is positioned midway between L1 and L2. The excitation coils are connected across a variable-frequency ac power supply as shown in Fig. 1(b). The oscillating magnetic field produced by the excitation coils is zero in the median plane of L3, and is proportional to the coordinate x for small values of x . The pick-up coil is connected to a lock-in amplifier [phase-sensitive detector (PSD)] which is used as the detector. The

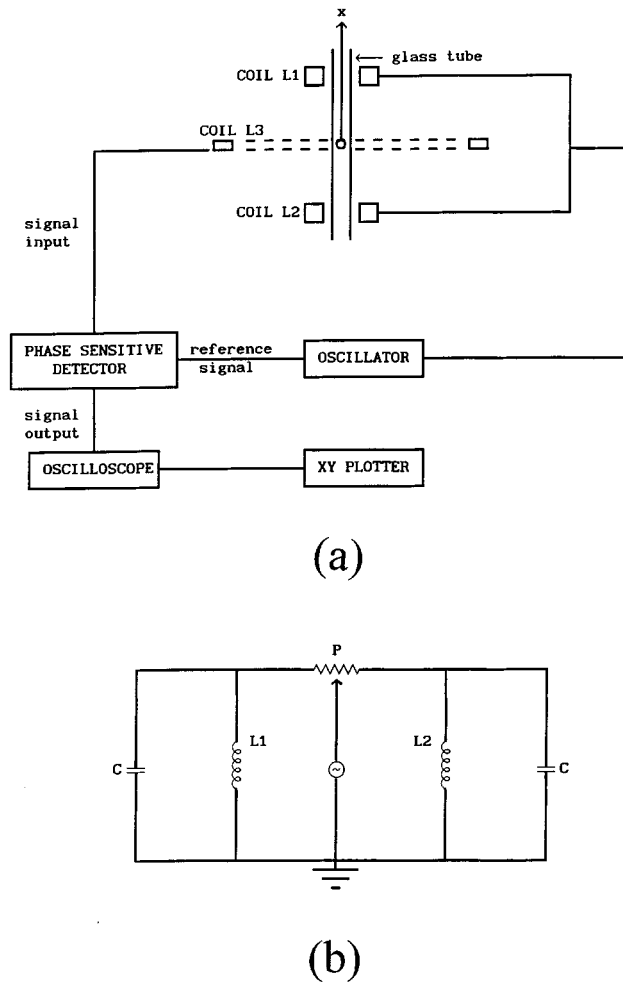


FIG. 1. (a) Block diagram of the circuit for measuring the position $x(t)$ of the steel ball. The origin of x is in the median plane of coil L3. The specification and parameters for the electrical and mechanical components are given in the Appendix. (b) Circuit for the excitation coils L1 and L2 showing the two LC loops and the potentiometer P .

output from the PSD is displayed on a digital oscilloscope and recorded on an XY plotter.

The PSD was nulled with the steel ball at 0. With the ball at a position x , a dc output is produced by the PSD. This output has two characteristics: (i) Its polarity is determined by the phase setting of the PSD and the sense of the ball's displacement. (ii) It is proportional to x if $|x| \leq 5$ cm, and becomes nonlinear, rising rapidly above the linear value, if $|x| > 5$ cm. The output in the linear region was calibrated by measuring the position of the ball as a function of the PSD output. This method of detecting the position of the ball is analogous to the operation of a linear-voltage-displacement transducer. (The position of any small conducting object inside the tube can be measured by this method.)

To achieve maximum sensitivity, the frequency f of the oscillator was set to the resonant frequency of the two LC loops shown in Fig. 1(b). Large branch currents flow through the excitation coils whilst maintaining a low feed current from the oscillator. Throughout this work, $f = 32.6$ kHz. The component P represents a 100Ω wire-wound potentiometer which was used as a coarse adjustment in phasing the PSD.

This facility is required to compensate for small errors which might occur in positioning the pick-up coil L3 midway between coils L1 and L2. Typically P was set close to its center. Specifications of the various electrical and mechanical components used in our experiment are given in the appendix.

We wish to study the oscillations of the gas at various frequencies, and according to Eq. (9) this can be done by varying the volume of gas V . A simple method of doing this is to partially fill the aspirator with a liquid [12]. The volume of gas is $V = V_0 - V_L$, where V_0 is the volume when the aspirator is empty and V_L is the volume of liquid. Then Eq. (9) can be written

$$T^2 = \frac{4\pi^2 m}{KA^2} (V_0 - V_L). \quad (10)$$

Thus for oscillations of a given type, a plot of T^2 versus V_L should yield a straight line with slope $-4\pi^2 m / KA^2$ and intercept V_0 , where K is the bulk modulus for these oscillations. This technique has been used to measure γ of air, using water as a filler and assuming the oscillations are adiabatic [12].

In our work, we have used both vacuum pump oil (which has a very low saturated vapor pressure < 5 Pa) and water as the fillers. Measurements could be taken for volumes between about 0.13% and 22.96% ($= V_0$); the corresponding frequencies vary between about 8 and 0.5 Hz. Amplitudes of the displacement varied between 5 and about 0.01 cm; the corresponding fractional changes in volume varied from about 8×10^{-2} to 2×10^{-4} at the higher frequencies and from about 4×10^{-4} to 10^{-6} at the lower frequencies.

In these experiments it is essential that the ball and the tube are clean, and that there are no leaks in the system. To avoid leaks we used a stopper made from Polyacetyl in the aspirator, with an O-ring seal between the stopper and the tube. The air used in our measurements was synthetic/medical grade having the following specifications: O_2 $21 \pm 2\%$; balance N_2 ; $C_n H_m$ and $H_2O < 4$ ppm.

III. RESULTS

We first consider the results obtained using vacuum pump oil as the filler in the aspirator. In Figs. 2(a) and 2(b) we present a typical oscilloscope trace for the oscillations of a small volume of gas ($V = 0.71\%$). The initial amplitude (measured from the center of the ball) was nearly 4 cm. We have, for clarity, displayed the tail of the oscillation separately in Fig. 2(b) where the time scale is half that of Fig. 2(a).

Similarly, in Figs. 3(a) and 3(b), a typical trace is shown for the oscillations of a larger volume of gas ($V = 13.21\%$). Note that in Fig. 3(b) the displacements in the tail have been magnified tenfold. The periods of each of the cycles shown in Figs. 2 and 3 were measured with the aid of the "x-enlargement" facility for the horizontal axis of the digital oscilloscope, to display just one or two cycles on the screen. Then, by activating the "period calculation" feature of the oscilloscope, the periods of individual cycles were determined accurately, either from peak-to-peak measurements or from intercept measurements on the time axis.

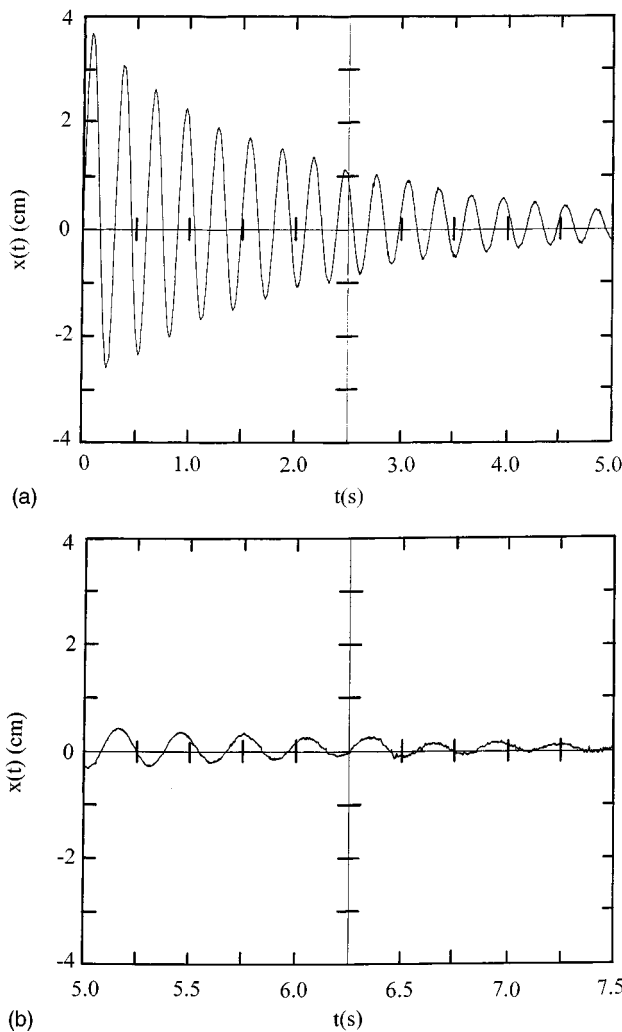


FIG. 2. (a) Oscilloscope trace for the position x of the steel ball versus t , for a volume of air = 0.71 l. The first sixteen cycles are shown. (b) As for (a), but with the time scale halved. Cycles 17–24 are shown.

Some examples taken from Fig. 3 are shown in Fig. 4. The first two cycles of Fig. 3(a) are shown in Fig. 4(a) and the third cycle and the first part of the fourth cycle of Fig. 3(b) are depicted in Fig. 4(b).

The results of measurements such as these are shown in Fig. 5 where the period T of a cycle is plotted against the number N of the cycle. The set of points labeled (a) are from Figs. 2(a) and 2(b); the points labeled (b) are from Figs. 3(a) and 3(b). It is clear that the two sets differ considerably. The periods of the higher frequency oscillation are essentially constant, $T = 0.300$ s (to within the resolution of the oscilloscope, ~ 2 ms) for all 22 cycles. By contrast, the plot for the oscillation with the longer period shows four distinct features, marked I–IV, in Fig. 5:

I. The first cycle has the lowest period, $T_a = 1.25$ s. This increases slightly in the next two cycles to 1.26 and then 1.27 s.

II. This is followed by a plateau of 4 cycles at $T_m = 1.27$ s.

III. At the end of the sixth or seventh cycle there is a rapid change, taking approximately three cycles, to a second plateau.

IV. The second plateau consists of five cycles at $T_i =$

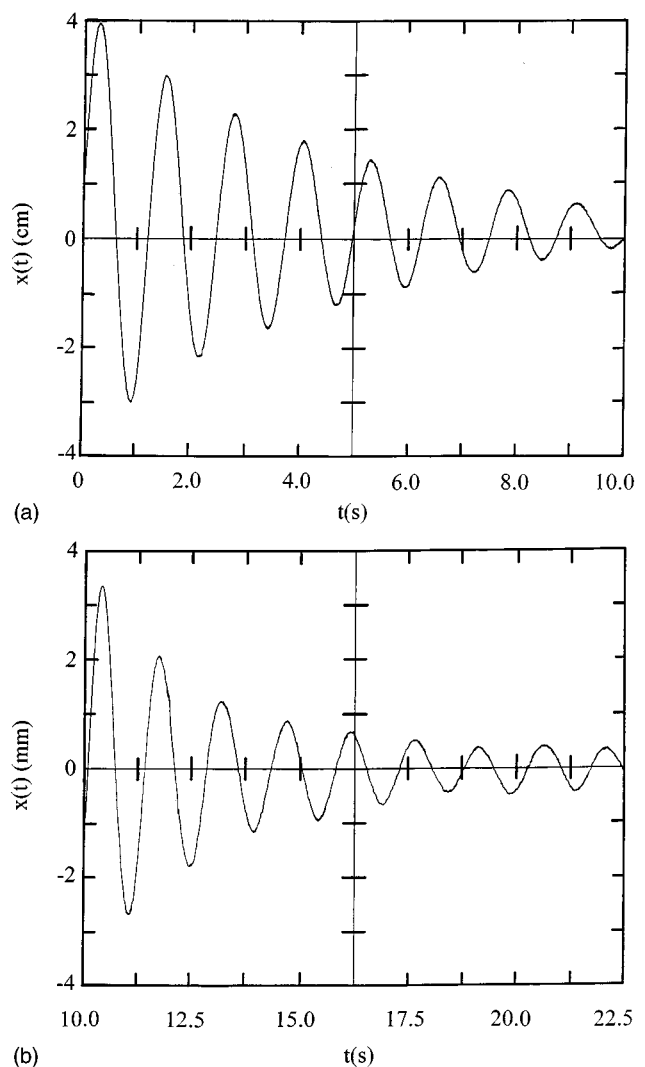


FIG. 3. (a) As for Fig. 2(a), but for a volume of air = 9.75 l. The first eight cycles are shown. (b) As for (a). Cycles 9–16 are shown. The vertical scale has been magnified tenfold.

1.50 s. (In fact, this plateau persists until the oscillations cease.)

The ratio of the largest to the smallest periods is $1.50/1.25 = 1.20$.

In Fig. 5 we have displayed just two sets of results for two different volumes of air. The results of a detailed study involving numerous measurements at other volumes show the following.

(i) When the volume of gas $V = V_0 - V_L$ is less than about 2 l, corresponding to $T \leq 0.5$ s, the measured values of T are of the type (a) in Fig. 5, with very little variation in T . (Actually, for V slightly below 2 l, a small increase in T is noticeable in the tail.)

(ii) For $T \geq 0.5$ s, the measured values are of the type (b) in Fig. 5, except that the ‘lip’ I could be reliably discerned only when $V \leq 6$ l, corresponding to $T \geq 0.9$ s. (It is not clear whether this ‘lip’ is absent at the higher frequencies or is not detected because of insufficient resolution in our measurements of T for $T \leq 0.9$ s.) The number of oscillations in the plateau II decreased as the volume of gas was increased, from 14 at the smallest volume to 4 at the larger volumes.

(iii) The measured values can be accurately reproduced.

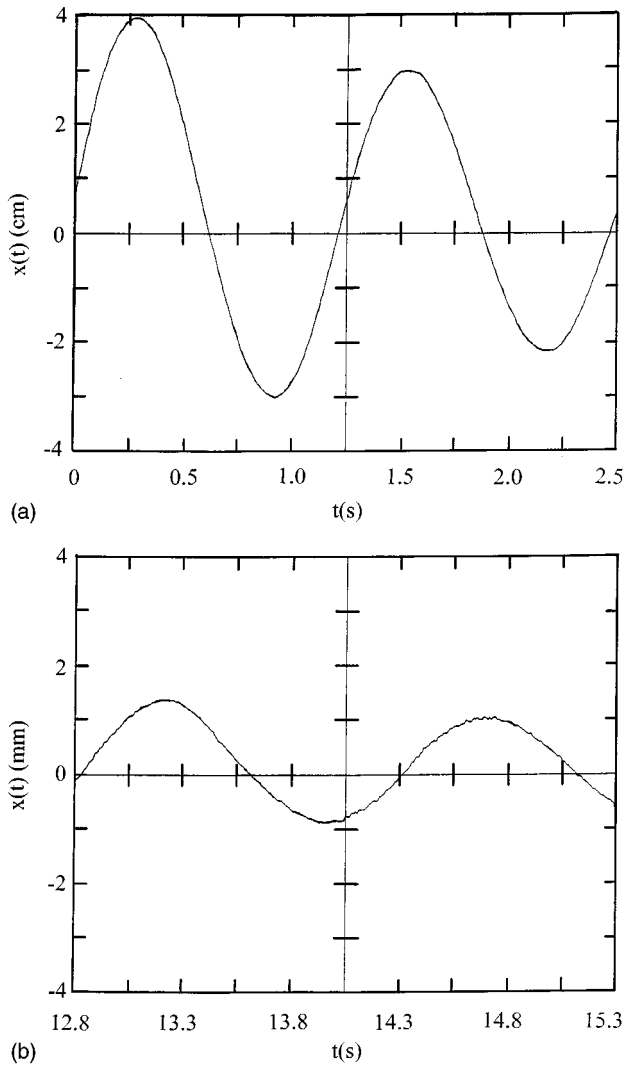


FIG. 4. (a) Enlargement of the first two cycles of Fig. 3(a) obtained using the "x-enlargement" facility of the oscilloscope. The measured peak-to-peak period is 1.25 s. (b) Enlargement of the third cycle and part of the fourth cycle of Fig. 3(b). The measured peak-to-peak period is 1.50 s.

Next, we consider a possible interpretation of results such as those shown in Fig. 5. The ratio $T_i/T_a = 1.2$ of the longest to the shortest periods in the plot (b) is close to the value for air of $\sqrt{\gamma} = 1.18$, which is just the expected ratio of the periods of isothermal and adiabatic oscillations (see Sec. I). This suggests the hypothesis that the first cycle in (b) is adiabatic and the cycles in the plateau IV are isothermal: the other oscillations are then presumed to be intermediate between these extremes. The oscillations in (a) are shown in Sec. IV to be intermediate.

To test these ideas we have extracted from plots such as Fig. 5 the values of T_a , T_i , and T_m for a range of values of V between 22.96% ($=V_0$, the equilibrium volume of gas when the aspirator is empty) and $V=0.13\%$ (the smallest volume for which a reliable trace could be obtained). Then, following the discussion in Sec. I, we have plotted T_a^2 , T_i^2 , and T_m^2 versus the volume of oil $V_L = V_0 - V$. These plots are shown in Fig. 6, where the straight lines were obtained by a least-mean-squares fit to the data. The intercepts on the V_L

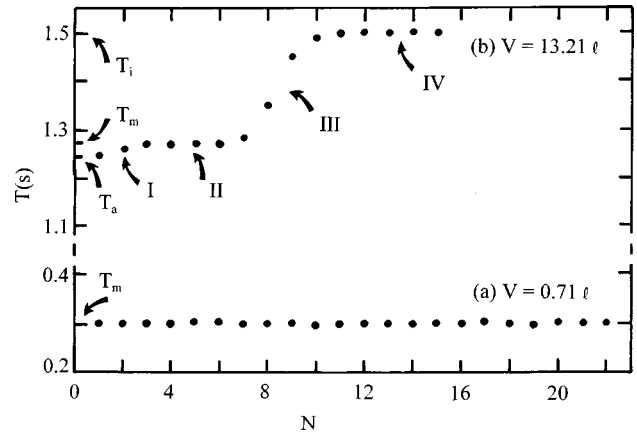


FIG. 5. The measured period T of a cycle versus the number N of that cycle. The set of points labeled (a) were obtained from Figs. 2(a) and 2(b) as described in the text. The set of points labeled (b) were obtained from Figs. 3(a) and 3(b).

axis and the slopes obtained from these straight lines are listed in Table I. Note that the values of V_0 given by the intercepts are all close to the measured volume of the empty aspirator plus the volume of the tube up to the equilibrium position of the ball, $V_0 = 22.96\%$. The equilibrium pressure of the gas during these measurements was $P = 95263$ Pa, being the sum of the atmospheric pressure 94459 Pa and the pressure $mg/A = 804$ Pa due to the ball. Also listed in Table I are values of the bulk moduli divided by the pressure K/P deduced from the measured slopes dT^2/dV_L with the aid of Eq. (10) and using the parameters in the Appendix.

Theoretical values of K/P can be obtained using the standard equation of state [13]

$$\frac{P\bar{V}}{RT} = Z, \quad (11)$$

where \bar{V} is the molar volume, and

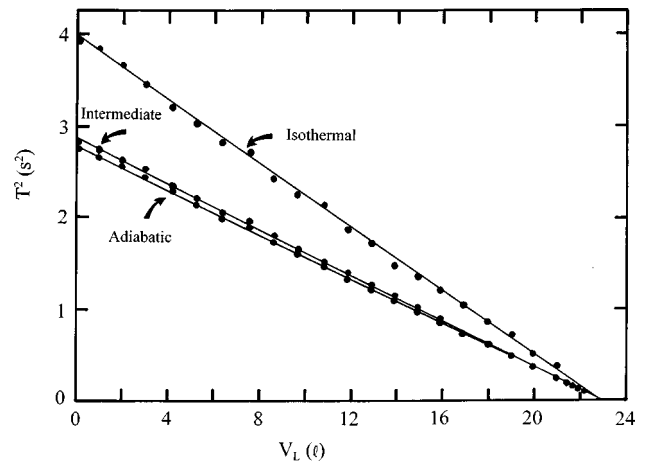


FIG. 6. The squares of the periods T_a , T_m , and T_i versus the volume of oil V_L in the aspirator. The values of T_a , T_m , and T_i were obtained from plots such as Fig. 5. The straight lines are least-mean-squares fits to the data.

TABLE I. Values of the intercepts and slopes obtained from the least-mean-squares fits in Fig. 6. Values of the bulk moduli were obtained from the slopes using Eq. (10) and the parameters given in the Appendix. $P = 95263$ Pa. The theoretical values of K_a/P , K_i/P and K_m/P , were obtained from Eqs. (13), (14), (37), and (40) as described in the text.

Experiment		Theory	
$V_0(\text{ℓ})$	$\frac{dT_a^2}{dV_L}(s^2\text{ℓ}^{-1})$	K_a/P	K_a/P
22.96	-0.1209 ± 0.005	1.395 ± 0.006	1.400
$V_0(\text{ℓ})$	$\frac{dT_i^2}{dV_L}(s^2\text{ℓ}^{-1})$	K_i/P	K_i/P
22.87	-0.1727 ± 0.001	0.976 ± 0.007	1.000
$V_0(\text{ℓ})$	$\frac{dT_m^2}{dV_L}(s^2\text{ℓ}^{-1})$	K_m/P	K_m/P
22.95	-0.1244 ± 0.008	1.355 ± 0.008	1.386

$$Z = 1 + \frac{B(T)}{\bar{V}} \quad (12)$$

is the compressibility factor. Then

$$K_i/P = Z. \quad (13)$$

Also, the adiabatic bulk modulus is given by the thermodynamic identity [14] $K_a = \gamma K_i$ and so

$$K_a/P = \gamma Z. \quad (14)$$

For air under the conditions of our experiment $\gamma = 1.40$. Also, the term B/\bar{V} in Eq. (12) is of order [13] -0.02% , which is too small to be measured in our experiment: consequently for the entries in the last column of Table I we have taken $Z = 1$ in Eqs. (13) and (14). We see that the theoretical and experimental values of K_a/P are in good agreement. For K_i/P the measured value in Table I is 2.4% below the theoretical value 1.000. The reason for this small discrepancy is not clear. The theoretical value of K_m/P in Table I is discussed in the next section.

We have also determined the relaxation time τ_m of the intermediate oscillations, such as those in the plateau II of Fig. 5 [i.e., the third to seventh cycles in Fig. 3(a)] by taking the ratio of successive amplitudes and using Eq. (7). For volumes of air below 2ℓ , where all the oscillations are intermediate, we have used ratios from traces such as Fig. 2(a). (We remark that if amplitudes larger than about 5 cm are used then the nonlinearity in the method for measuring $x(t)$ (see Sec. II) leads to large errors in the measured relaxation time.) The results are shown in Fig. 7, where τ_m is plotted against the measured period T of the oscillations. The solid curve in Fig. 7 is discussed in the next section. We have attempted to obtain values of τ in the transition region III and in the isothermal tail IV of Fig. 5, but these showed considerable variability. Values of τ in the transition III are

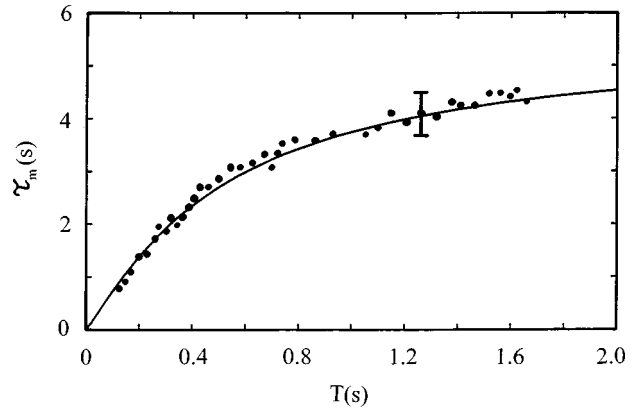


FIG. 7. The relaxation time for intermediate oscillations versus the period T . The measured values were obtained as described in the text. The solid curve is given by Eq. (41) with $B = 12s^{-1/6}$ and $C = 2.2s^{-7/6}$.

smaller than τ_m , varying between ~ 0.5 and $0.8\tau_m$. Values of τ in the isothermal tail tended to be longer than τ_m , sometimes by as much as a factor 2. It is not feasible to obtain a meaningful value of τ for the initial adiabatic oscillation [such as the first oscillation in Fig. 3(a)].

The preceding results were obtained using vacuum pump oil to vary the volume of air in the aspirator. It is also interesting to use water for this purpose. A plot of the various measured periods versus the volume of water is shown in Fig. 8, and values of the intercepts and slopes are given in Table II. To analyze these results we suppose that the saturated vapor pressure of the water makes no contribution to the bulk modulus of air. Then the equilibrium pressure to be used in evaluating the various bulk moduli is the atmospheric pressure 94259 Pa, minus the saturated vapor pressure of water 2064 Pa at 18°C , plus the pressure 804 Pa due to the ball. We also suppose that heat released by condensation of some vapor during the compression part of a cycle is absorbed at the liquid-vapor interface and does not affect the compression of the gas. Similarly during the expansion part of a cycle. (Any latent heat absorbed by the air would increase the temperature changes of the adiabatic oscillations; one can readily show that such enhancement cannot exceed

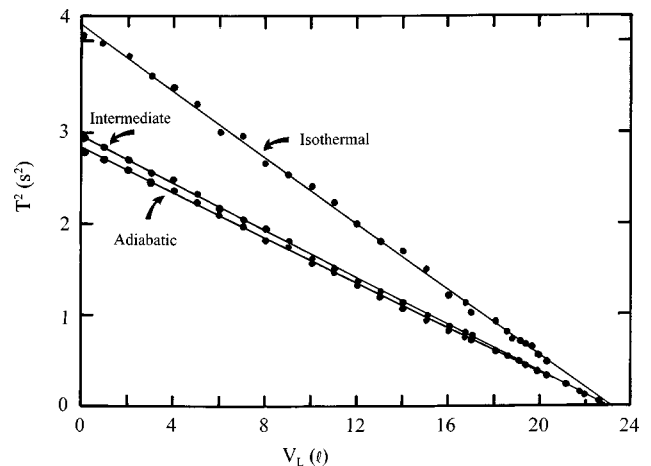


FIG. 8. As for Fig. 6 but with water used to vary the volume of air in the aspirator.

TABLE II. As for Table I but with water instead of vacuum pump oil in the aspirator. $P=92999$ Pa.

	Experiment		Theory
$V_0(\text{cm})$	$\frac{dT_a^2}{dV_L}(s^2\text{cm}^{-1})$	K_a/P	K_a/P
22.84	-0.1234 ± 0.0004	1.400 ± 0.005	1.398
$V_0(\text{cm})$	$\frac{dT_i^2}{dV_L}(s^2\text{cm}^{-1})$	K_i/P	K_i/P
23.10	-0.1795 ± 0.0014	0.962 ± 0.008	1.000
$V_0(\text{cm})$	$\frac{dT_m^2}{dV_L}(s^2\text{cm}^{-1})$	K_m/P	K_m/P
22.84	-0.1291 ± 0.0005	1.337 ± 0.005	1.386

20%.) Values of the bulk moduli divided by P , obtained from the measured slopes and Eq. (10), are listed in Table II, together with the corresponding theoretical values for isothermal and adiabatic oscillations obtained from Eqs. (13) and (14) with $Z=1$. For γ we have used [2] $\gamma=(7+h)/(5+h)$, where h (the fraction of molecules that are H_2O) is 0.022 for a saturated vapor at 18°C . Again there is good agreement between the experimental and theoretical values of K_a/P , while the measured value of K_i/P is again a little lower than the theoretical value. The theoretical value of K_m/P in Table II is discussed below.

We made a separate set of measurements to check the value of K_i/P and the assumed lack of effect of the saturated vapor pressure of water. With dry air at a pressure $P=95263$ Pa in an empty aspirator we obtained for an average of 80 measurements $T_i=2.000$ s. With saturated water vapor at 23.5°C in the aspirator (partial pressure of air=92454 Pa) the average was $T_i=2.028$ s. The ratio 1.014 of these periods is in excellent agreement with the square root of the inverse ratio of the pressures $(95263/92454)^{1/2}=1.015$, as required by Eq. (9) with $K_i \sim P$. Also, the values of K_i/P calculated from Eq. (9) (and using $V=22.96\text{cm}^3$ and the data in the Appendix) are 0.965 for dry air and 0.970 for air plus saturated water vapor, in good agreement with the values in Tables I and II.

The results shown in Figs. 2–8 are for an initial displacement of 4 cm. We have also made measurements with smaller initial displacements, down to 0.5 cm. In all cases an isothermal “tail” was present in the plot of $x(t)$ versus t .

IV. THEORETICAL MODEL

We present a model for the effects of heat flow within the gas on the bulk modulus of the gas and the relaxation time of the oscillations. This model is intended to apply only to the initial departure from adiabatic oscillations; that is, to intermediate oscillations with constant period, such as those in the plateau II in Fig. 5.

Consider first the damping force (5). In general, there will be contributions to this force from (i) friction due to motion of the ball in the tube, (ii) viscous effects in the bulk of the

gas, and (iii) heat flows in the gas. Because the dimensions of our container are small compared to the wavelength of sound at the frequencies we use (Sec. I), viscous damping in the bulk of the gas will be small. Also, it is helpful to start by considering an idealized experiment in which there is no friction in the tube. Then the only dissipation is due to thermal conduction in the gas. Consequently, if the oscillations are adiabatic, the damping force is zero, and in Eq. (7) $\tau=\infty$, so that

$$x(t)=X\cos(2\pi t/T). \quad (15)$$

Due to the finite thermal conductivity of the gas and the container, the oscillations cannot be perfectly adiabatic, and we ask how the heat flows alter the bulk modulus (14) and the relaxation time τ .

Our analysis follows closely that of Clark and Katz [15] who estimated the corrections that must be made for non-adiabatic compressions in a resonance method for determining the ratio of specific heats of a gas. The experiment to which they applied their results differs from ours: they consider a driven oscillator (a piston in a horizontal tube with a gas on both sides of the piston contributing to the restoring force) and study the resonance curve. For this reason, and also to correct certain errors in their calculations, it is helpful to present a brief outline of their analysis.

We start by writing the temperature of the gas as [15]

$$\theta=\theta_0-(MC_v)^{-1}P\Delta V+\theta_D(\mathbf{r},t), \quad (16)$$

where θ_0 is the ambient temperature, M is the mass of gas, and P is the equilibrium pressure of the gas. The unknown function θ_D , which represents the departure from the temperature of an adiabatic oscillation, must satisfy [15]

$$\partial\theta_D/\partial t=\gamma\kappa\nabla^2\theta_D, \quad (17)$$

where κ is the thermal diffusivity of the gas [2]. [In arriving at Eqs. (16) and (17) it is assumed that changes in the pressure, density, thermal conductivity, and specific heat of the gas from their equilibrium values may be neglected.]

To solve Eq. (17) one considers a spherical container of radius R . The temperature of the gas is assumed to be spherically symmetric, so that $\theta_D=\theta_D(r,t)$. It is assumed that the temperature of the gas close to the wall is equal to θ_0 , and that the temperature at the center of the sphere is finite: then the boundary conditions are

$$\theta_D=(MC_v)^{-1}P\Delta V \quad \text{at } r=R \quad (18)$$

and

$$\theta_D \quad \text{finite at } r=0. \quad (19)$$

A solution to Eq. (17) which satisfies Eq. (19) is

$$\theta_D=\frac{D}{r}[e^{r/a}\cos(bt+r/a+\nu)-e^{-r/a}\cos(bt-r/a+\nu)], \quad (20)$$

where D , a , b , and ν are constants, and

$$b=2\gamma\kappa/a^2. \quad (21)$$

The boundary condition (18) with $\Delta V = Ax$ and x given by Eq. (15) requires

$$(i) \quad b = 2\pi/T. \quad (22)$$

It is helpful to digress here: from Eqs. (21) and (22) the length scale a is given by

$$a = (\gamma\kappa T/\pi)^{1/2}. \quad (23)$$

It turns out that in our experiment

$$a \ll R \quad (24)$$

[see Eq. (44)], and consequently in requiring that Eq. (20) satisfy Eq. (18) we may neglect terms of order unity and of order $e^{-R/a}$ in comparison with $e^{R/a}$. Then

$$(ii) \quad \cos\nu = \cos R/a, \quad (25)$$

$$\sin\nu = -\sin R/a, \quad (26)$$

and

$$D = (PAXR/MC_v)e^{-R/a}. \quad (27)$$

The average value of θ_D in the sphere is given by

$$\bar{\theta}_D = (4\pi R^3/3)^{-1} \int_0^R \theta_D 4\pi r^2 dr. \quad (28)$$

Substituting Eq. (20) in Eq. (28) and using Eqs. (24)–(27), we find

$$\bar{\theta}_D \approx (3PAX/2MC_v)(a/R)[\cos(2\pi t/T) + \sin(2\pi t/T)]. \quad (29)$$

[Note that $\bar{\theta}_D$ lags $x(t)$ by 45° .] Using Eq. (15), the last parenthesis in Eq. (29) can be expressed in terms of x and \dot{x} . It is also helpful to use the thermodynamic relation [15]

$$P = (\gamma - 1)MC_v \left(\frac{\partial \bar{\theta}}{\partial V} \right)_P. \quad (30)$$

Then

$$\bar{\theta}_D = \frac{3}{2}(\gamma - 1)A \left(\frac{\partial \bar{\theta}}{\partial V} \right)_P (a/R) \left(x - \frac{T}{2\pi} \dot{x} \right). \quad (31)$$

From Eqs. (16), (30), and (31) the departure of the temperature of the gas from the ambient value θ_0 , averaged over the volume of the sphere, is

$$\Delta \bar{\theta} = -(\gamma - 1)A \left(\frac{\partial \bar{\theta}}{\partial V} \right)_P \left[\left(1 - \frac{3a}{2R} \right) x + \frac{3aT}{4\pi R} \dot{x} \right]. \quad (32)$$

The total pressure change associated with a temperature and volume change is

$$\Delta P = \left(\frac{\partial P}{\partial \bar{\theta}} \right)_V \Delta \bar{\theta} + \left(\frac{\partial P}{\partial V} \right)_{\bar{\theta}} \Delta V. \quad (33)$$

Substituting Eq. (32) in Eq. (33) and using the relation

$$\left(\frac{\partial P}{\partial \bar{\theta}} \right)_V \left(\frac{\partial \bar{\theta}}{\partial V} \right)_P = - \left(\frac{\partial P}{\partial V} \right)_{\bar{\theta}} = (\gamma V)^{-1} K_a,$$

where K_a is the adiabatic bulk modulus, we find that

$$\Delta P = \Delta P_x + \Delta P_{\dot{x}}. \quad (34)$$

Here

$$\Delta P_x = - \left(1 - \frac{3(\gamma - 1)a}{2\gamma R} \right) K_a \Delta V/V \quad (35)$$

and

$$\Delta P_{\dot{x}} = - \frac{3(\gamma - 1)K_a A a T}{4\pi\gamma V R} \dot{x}. \quad (36)$$

Equations (35) and (36) are the desired results which we wish to apply to our experiment: similar results were first obtained by Clark and Katz [15]. From Eq. (35) the bulk modulus for intermediate oscillations is

$$K_m = \left(1 - \frac{3(\gamma - 1)a}{2\gamma R} \right) K_a. \quad (37)$$

Also, the damping force associated with heat conduction is $A\Delta P_{\dot{x}} = -\beta_c \dot{x}$. Hence we obtain from Eq. (36)

$$\beta_c = \frac{3(\gamma - 1)K_a A^2 a T}{4\pi\gamma V R}. \quad (38)$$

So far we have neglected friction due to motion of the ball in the tube. We assume that this force has the form $-\beta_0 \dot{x}$, where β_0 is a constant. Then the total damping force is given by Eq. (5) with $\beta = \beta_0 + \beta_c$, and the relaxation time (8) for intermediate oscillations is

$$\tau_m = m/2(\beta_0 + \beta_c). \quad (39)$$

To compare Eqs. (37)–(39) with experiment, we first express these results in terms of the period T . Consider the ratio a/R . Using Eq. (23), $R = (3V/4\pi)^{1/3}$ and Eq. (9) to eliminate the volume V we obtain

$$\frac{a}{R} = \left(\frac{\gamma\kappa}{\pi} \right)^{1/2} \left(\frac{16\pi^3 m}{3\gamma P A^2} \right)^{1/3} T^{-1/6}. \quad (40)$$

Using Eqs. (38), (40), and (9) in Eq. (39) we find that τ_m can be expressed in the form

$$\tau_m = \frac{BT^{7/6}}{1 + CT^{7/6}}. \quad (41)$$

Here B and C are constants (independent of T):

$$B = \frac{\gamma}{6\pi(\gamma - 1)} \left(\frac{\pi}{\gamma\kappa} \right)^{1/2} \left(\frac{3\gamma P A^2}{16\pi^3 m} \right)^{1/3} \quad (42)$$

and

$$C = (2\beta_0/m)B. \quad (43)$$

Equation (37) and Eqs. (40)–(43) are the main results of this section: they provide an estimate for the effects of conduction on the bulk modulus and the relaxation time.

Using the data given earlier and $\kappa \approx 2 \times 10^{-5} \text{ m}^2 \text{ s}^{-1}$ for air at 18 °C, Eq. (40) yields

$$\frac{a}{R} \approx 2.4 \times 10^{-2} T^{-1/6}. \quad (44)$$

For our experiment, $T^{-1/6}$ is nearly unity: it varies slowly from about $0.9 \text{ s}^{-1/6}$ to $1.4 \text{ s}^{-1/6}$. Thus the correction to the adiabatic bulk modulus in Eq. (37) is approximately 1% compared with a measured difference of about 2.5%, see Table I. Next, we consider the relaxation time. We first comment that the dependence of τ_m on T given by Eq. (42) can reproduce the experimental results very well, as illustrated in Fig. 7, where the solid curve is a plot of Eq. (42) with $B = 12 \text{ s}^{-1/6}$ and $C = 2.2 \text{ s}^{-7/6}$. The value of B computed from Eq. (42) is about 30% lower than this, $B \approx 8 \text{ s}^{-1/6}$. We are unable to compare the value of C with Eq. (43) because the value of β_0 is unknown. It is interesting to note that the departure from an approximately linear relationship between τ_m and T in Fig. 7 is a manifestation of the friction in the tube. [If this friction is negligible, then β_0 , and hence $C \approx 0$, and Eq. (41) becomes $\tau_m \approx BT^{7/6}$.]

Finally, we return to the question of whether the oscillations at frequencies above about 2 Hz are adiabatic or intermediate. These are oscillations such as those in Fig. 2 for which there is no significant variation in period with decreasing amplitude (see Fig. 5). Here it is difficult to distinguish between adiabatic and intermediate oscillations from measurements of the period alone (see Figs. 6 and 8, where the adiabatic and intermediate lines approach each other as $T \rightarrow 0$). A more sensitive test is provided by the measurements of τ_m . The fact that these values agree with Eq. (41) as $T \rightarrow 0$ (see Fig. 7) means that the corresponding oscillations are intermediate: for adiabatic oscillations $\beta_c = 0$ in Eq. (39) and $\tau = m/2\beta_0$ is independent of T .

The above model applies to the intermediate oscillations with constant period. We have not attempted a theoretical description of the transition regions, such as I and III in Fig. 5, where the period is changing. One may speculate that the transition I from an adiabatic oscillation is associated with a transient during which the nonuniform temperature distribution θ_D in Eq. (16) is established. The reason for the large transition III to an isothermal mode, which occurs when the amplitude is sufficiently small, is not clear.

V. DISCUSSION

We have used a modification of Rüchardt's experiment to study oscillations in air confined to a finite volume at room temperature and pressure. The dimensions of the container

are small compared to the wavelength of sound for the frequencies used (0.5–8 Hz). Our results indicate that the nature of these oscillations depends on both the frequency and the amplitude of the oscillation. Above about 2 Hz the oscillations are intermediate, to within the accuracy of our measurements. For frequencies below 2 Hz the oscillations are observed to undergo several changes as their amplitude decreases due to damping. There is (i) an initial adiabatic oscillation (lasting roughly one cycle), followed by (ii) a transition (lasting one or two cycles) to intermediate oscillations which persist for several cycles, until (iii) the amplitude has decreased to a few mm when there is a second, larger, transition (lasting two or three cycles), to (iv) isothermal oscillations which persist until the oscillations cease. In this second transition the damping is observed to increase. Some of these features are strongly reminiscent of Stokes' analysis [3] (see Sec. I) of changes between adiabatic and isothermal oscillations in gases, and perhaps one may think of the frequency below which isothermal oscillations are observed in a confined gas as the "Stokes limit."

We have also presented an approximate model for the effects of heat conduction on the bulk modulus and the relaxation time for the initial intermediate oscillations. The results of this model [Eqs. (37) and (41)] are in qualitative agreement with the measured values but they underestimate the effect of conduction on the bulk modulus and overestimate its effect on the dissipation.

Note added in proof. Measurements of the initial amplitude of the isothermal tail as a function of the volume of gas show that this amplitude increases as the volume increases. We have succeeded in improving the quality of the isothermal tail sufficiently that accurate measurements of the relaxation time in the tail can be performed. These measurements will be presented elsewhere.

ACKNOWLEDGMENTS

We acknowledge financial support received from the South African Foundation for Research and Development, and technical assistance from Guy Dewar, Johnny Wilsenach, and Karl Penzhorn.

APPENDIX

Specification and parameters for the electrical and mechanical components in Fig. 1 are listed below:

Oscillator: Philips PM5141.

Digital Oscilloscope: Philips PM3350A.

Phase-sensitive Detector: PAR Model 5101.

XY Plotter: HP Model 2DR2M.

Coils L1 and L2: Each 100 turns. Resistance 1.8 Ω . Inductance $L1=L2=256 \mu\text{H}$.

Mean diameter=24 mm. Height=14 mm.

Coil L3: 800 turns. Resistance 16.2 Ω . Inductance $L3=39.3 \text{ mH}$. Mean diameter 125 mm. Height 11 mm.

Separation of L1 and L2=16 cm.

Capacitors: $C = 100 \text{ nF}$ (nominal).

Glass tube and steel ball acquired from Leybold Didactic GMBH (Catalogue number 37105). Tube diameter=16.0025 mm. Mass of ball=16.5 g.

Schott Glass Aspirator: 20/ (nominal).

- [1] S. G. Brush, *The Kind of Motion We Call Heat* (North-Holland, Amsterdam, 1976), Vol. 1, Chap. 3.
- [2] See, for example, A. D. Pierce, *Acoustics* (McGraw-Hill, New York, 1981), Chap. 1.
- [3] G. G. Stokes, *Philos. Mag.* **1**, 305 (1851).
- [4] M. Bailyn, *A Survey of Thermodynamics* (AIP, NY, 1994), p. 52.
- [5] See, for example, A. L. Fetter and J. D. Walecka, *Theoretical Mechanics of Particles and Continua* (McGraw-Hill, New York, 1980), Chap. 12.
- [6] See, for example, B. S. Massey, *Mechanics of Fluids* (Van Nostrand, London, 1970); R. M. Rotty, *Introduction to Gas Dynamics* (Wiley, New York, 1962).
- [7] J. R. Partington and W. G. Shilling, *The Specific Heats of Gases* (Ernest Benn, London, 1924), p. 52.
- [8] P. M. Morse, *Vibration and Sound* (McGraw-Hill, New York, 1948), Chap. 7.
- [9] E. Ruchardt, *Phys. Z.* **30**, 58 (1929).
- [10] R. Rinkel, *Phys. Z.* **30**, 805 (1929).
- [11] P. H. Brodersen, *Z. Phys.* **62**, 180 (1930).
- [12] C. G. Deacon and J. P. Whitehead, *Am. J. Phys.* **60**, 859 (1992).
- [13] J. H. Dymond and E. B. Smith, *The Virial Coefficients of Gases* (Clarendon, Oxford, 1969).
- [14] E. A. Guggenheim, *Thermodynamics* (North-Holland, Amsterdam, 1950), p. 101.
- [15] A. L. Clark and L. Katz, *Can. J. Res.* **18**, 23 (1940).